

Supporting Information

***In situ* activation of COOH-functionalized ZIF-90-enabled reductive CO₂ N-formylation**

Kaixun Zhu, Yuncong Li, Zhengyi Li, Yixuan Liu, Hongguo Wu* and Hu Li*

Supplementary Text

Tables and Figures

Table S1. Crystallinity and crystallite size of ZIF-90 and ZIF-90-C.

Table S2. Surface area and porosity of ZIF-90 and ZIF-90-C.

Table S3. Elemental analysis of ZIF-90 and ZIF-90-C.

Table S4 The polarity (π^*) of different solvents.

Table S5 Catalytic activity of morpholine and CO₂ formylation under different silane conditions ^a.

Fig. S1 Synthesis schematic of carboxylic acid-functionalized ZIF-90-C.

Fig. S2 FT-IR spectra of ZIF-90 and ZIF-90-C.

Fig. S3 Pore size distribution of ZIF-90 and ZIF-90-C.

Fig. S4 SEM images: (a) ZIF-90, (b) ZIF-90-C; TEM images: (c) ZIF-90, (d) ZIF-90-C; AFM image: (e) ZIF-90-C; TEM-EDX image of (f) ZIF-90-C and elemental mapping images of (g) C, (h) O, (i) N, and (j) Zn present in ZIF-90-C.

Fig. S5 (a) XPS survey spectra of ZIF-90 and ZIF-90-C; (b) C 1s spectra of ZIF-90 and ZIF-90-C; (c) O 1s spectra of ZIF-90 and ZIF-90-C; and (d) Zn 2p spectra of ZIF-90 and ZIF-90-C.

Fig. S6 The N-formylation activity of CO₂ catalyzed by ZIF-90-C using different solvents.

Fig. S7 Effect of (a) catalyst amount, (b) temperature, (c) reaction time, and (d) PhSiH₃ loading on reductive of CO₂ with **1a** for synthesis of **1b** using ZIF-90-C. Reaction conditions: **1a**, 0.25 mmol; CH₃CN, 2 mL; [CO₂ balloon; PhSiH₃, 0.5 mmol; T, 50 °C; t, 24 h] for panel (a); [CO₂ balloon; 5 mol% catalyst; PhSiH₃, 0.5 mmol; t, 24 h] for panel (b); [CO₂ balloon; 5 mol% catalyst; PhSiH₃, 0.5 mmol; T, 50 °C] for panel (c); and [CO₂ balloon; 5 mol% catalyst; 0.5 mmol; T, 50 °C; t, 24 h] for panel (d).

Fig. S8 The mass spectrum of the PhSiH₃ aggregation.

Fig. S9 ¹H NMR spectrum of CO₂ hydrosilylation without an amine (solvent: DMSO-D₆).

Fig. S10 (a) Study on the recyclability of catalyst ZIF-90-C; (b) XRD patterns of fresh and reused ZIF-90-C after five cycles; (c) N₂ sorption isotherms of fresh and reused ZIF-90-C after five cycles and (d) FT-IR spectra of fresh and reused ZIF-90-C after five cycles.

Fig. S11 Energy distribution profiles of N-formylmorpholine and CO₂ reaction without catalyst.

Fig. S12 Energy distribution profiles of N-formylmorpholine and CO₂ reaction catalyzed by ZIF-90-C.

Fig. S13 The conversion rate of PhSiH₃ in PhSiH₃/CO₂-to-**B** at different reaction temperatures with (a) no catalyst and (b) ZIF-90-C; Kinetic plots of PhSiH₃/CO₂-to-**B** with (c) no catalyst and (d) ZIF-90-C; (e) Arrhenius profiles for PhSiH₃/CO₂-to-**B**; (f) ATR-FTIR spectra of PhSiH₃ before CO₂ absorption, after CO₂ absorption and ZIF-90-C treating with PhSiH₃. Reaction conditions: 5 mol% catalyst, 2.0 mL CH₃CN, 0.5 mmol PhSiH₃, and CO₂ balloon.

Fig. S14 HR-MS spectrum of ¹³C-labeled formoxysilane. Reaction conditions: ¹³CO₂ balloon, morpholine (0.25 mmol), PhSiH₃ (0.5 mmol), ZIF-90-C (5 mol%), CH₃CN (2.0 mL), 50 °C and 5 h.

Fig. S15 GC-MS spectrum of ¹³C-labeled N-formylmorpholine. Reaction conditions: ¹³CO₂ balloon, morpholine (0.25 mmol), PhSiH₃ (0.5 mmol), ZIF-90-C (5 mol%), CH₃CN (2.0 mL), 50 °C and 5 h.

Fig. S16 The mass spectrum of **2a**.

Fig. S17 The mass spectrum of **2b**.

Fig. S18 The mass spectrum of **2c**.

Fig. S19 The mass spectrum of **2d**.

Fig. S20 The mass spectrum of **2e**.

Fig. S21 The mass spectrum of **2f**.

Fig. S22 The mass spectrum of **2g**.

Fig. S23 The mass spectrum of **2h**.

Fig. S24 The mass spectrum of **2i**.

Fig. S25 The mass spectrum of **2j**.

Fig. S26 The mass spectrum of **2k**.

Fig. S27 The mass spectrum of **2l**.

Fig. S28 The mass spectrum of **2m**.

Fig. S29 The mass spectrum of **2n**.

Fig. S30 The mass spectrum of **2o**.

Experimental section

Materials

Materials: H₂O₂ (30wt % in water), and imidazole-2-carboxaldehyde (ICA,98%) were purchased from Alfa Aesar. Zn(NO₃)₂·6H₂O (98%) was purchased from MACKLIN reagent Co., Ltd. Morpholine (99%), benzylamine (99%), N-methylaniline (99%), and N-formylmorpholine (99%) were purchased from Shanghai Aladdin Reagent Co., Ltd. CH₃CN (99%), CH₃OH (99%), CH₃CH₂OH (99%), N,N-dimethylformamide (DMF, 99%), tetrahydrofuran (THF, 99%), ethyl acetate (99%), and *n*-hexane (99%) were bought from Beijing Innochem Sci.&Tech.Co.Ltd. All solvents were analytical reagent and used without further purification. All silanes and other reagents were purchased from TCI Reagent Co., Ltd. (Shanghai).

The synthesis of catalysts

First, Zn(NO₃)₂·6H₂O (0.202 g) and imidazole-2-carboxaldehyde (ICA) (0.223 g) were dissolved in DMF (50 mL) (solution 1) and DMF (25 mL) (solution 2), respectively. Then, solution 1 and solution 2 were mixed. DMF (25 mL) containing triethylamine (0.26 mL) (solution 3) was then poured into the mixture of solution 1 and 2 and stirred for 3 min, followed by adding methanol (50 mL) to stop the reaction. Finally, the yellow precipitate (ZIF-90) was collected by centrifugation, washed with ethanol (30 mL x 3), and centrifuged at 9000 rpm for 5 min. Then, it was vacuum-dried at 70 °C for 36 h. The extracted ZIF-90 (0.10 g) was then suspended in deionized water (30 mL). H₂O₂ (0.32 mL) dissolved in deionized water (15 mL) was slowly added to the suspended ZIF-90 mixture and reacted at room temperature for 24 h, followed by centrifugation at 9000 rpm for 10 min and vacuum-drying at 70 °C for 24 h to obtain the solid catalyst (ZIF-90-C).

Catalytic reaction

All N-formylation reactions were carried out in a 15 mL Schlenk tube with an inner connector in CO₂ (99.99%) environment. In general procedure, ZIF-90-C (5 mol%) was placed in a Schlenk tube, and then the reaction tube was vacuumed by mechanical pump and fixed by magnetic stirrer. Amines (0.25 mmol) and CH₃CN (1 mL) were added to the syringe and put into the reaction tube. Then the CO₂ balloon was introduced into the vacuum reactor and connected with the inner spiral tube. After 30 min, hydrosilane (0.5 mmol) and CH₃CN (1 mL) were added to the syringe, and the resulting mixture was stirred at 500 rpm at 50 °C for 24 h. After the reaction, the liquid was

filtered by syringe filter (0.22 μm), and further identified by gas chromatography (GC) and gas chromatography-mass spectrometry (GC-MS).

Catalyst recycling study

The reusability test of ZIF-90-C was carried out under the optimal reaction conditions (50 $^{\circ}\text{C}$ for 24 h), namely N-formylmorph (0.25 mmol), PhSiH_3 (0.5 mmol), ZIF-90-C (5 mol%), CH_3CN (2.0 mL), and CO_2 balloon. After each reaction cycle, ZIF-90-C catalyst was separated from the reaction system by centrifugation, washed with methanol (15 mL \times 3) and vacuum dried at 70 $^{\circ}\text{C}$ for 12 h. The recovered catalyst was then applied directly to the next reaction.

Isotopic labeling experiments

$^{13}\text{CO}_2$ was prepared by addition of 20 mL HCl (1.8 M) into 20 mL Na_2CO_3 - ^{13}C (1.0 M) aqueous solution at 40 $^{\circ}\text{C}$ stirring for 25 min, and collected with a balloon. In a general procedure, ZIF-90-C (5 mol%) was placed in a Schlenk tube, and then the reaction tube was vacuumed by mechanical pump and fixed by magnetic stirrer. Amine (0.25 mmol) and CH_3CN (1 mL) were taken with a syringe and then put into the reaction tube. Then the $^{13}\text{CO}_2$ balloon was introduced into the vacuum reactor and connected with the inner spiral tube. After reaction 30 min, hydrosilane (0.5 mmol) and CH_3CN (1 mL) were added with the syringe, and the resulting mixture was stirred at 500 rpm at 50 $^{\circ}\text{C}$ for 5 h. After the reaction, the liquid was filtered by syringe filter (0.22 μm), and further identified by gas chromatography-mass spectrometry (GC-MS) and high resolution mass spectrum (HR-MS).

Catalyst characterization

Scanning electron microscope (SEM) images were obtained by operating ZEISS SIGMA300 instrument under 10 kV vacuum. Transmission electron microscopy (TEM) was performed on TALOS F200C. Images of atomic force microscopy (AFM) were obtained by Bruker Innova IRIS. The fourier transform infrared (FT-IR) spectra of solid samples were performed on the NICOLET iS50 (Thermo) spectrometer using KBr particles coupled with the iS50 ATR (Attenuated Total Reflectance) attachment. The X-ray powder diffraction (XRD) patterns were obtained by Bruker D8 Advance under the conditions of Cu Ka radiation and 2θ scanning at 5 $^{\circ}$ -90 $^{\circ}$. X-ray photoelectron spectroscopy (XPS) was obtained by Nexsa spectrometer, and the data were fitted by XPSPEAK software. Gas adsorption experiments were carried out by ASAP 2460 equipment (powder technology) at 77 K in N_2 , 273 K in CO_2 and 323 K. The specific surface area

were obtained by Brunauer-Emmett-Teller (BET) method. And average pore size of the catalyst were obtained by Horvath-Kawazoe (HK) and Barrett-Joyner-Halenda (BJH) methods. Isothermic heat of adsorption (Q_{st}) for CO_2 was calculated using Clausius-Clapeyron equation:

$$Q_{st} = \frac{RT_1T_2 \ln\left(\frac{p_2/p_1}{T_2/T_1}\right)}{T_2 - T_1}$$

Two sets of adsorption data were collected at two different temperatures: P = equilibrium pressure (mm Hg), different pressures under the same adsorption capacity, T = temperature (K), and $R = 0.00831 \text{ kJ}\cdot\text{mol}^{-1} \text{ K}^{-1}$.

The yield of naphthalene was determined by GC-MS and GC (Agilent 7890B). The calculation formula of yield and conversion rate were as follows:

$$\text{Conversion (\%)} = \left(1 - \frac{\text{mole of residual substrate}}{\text{mole of initial substrate}}\right) \times 100\%$$

$$\text{Yield (\%)} = \frac{\text{mole of product}}{\text{mole of initial substrate}} \times 100\%$$

CHN and O elements were analyzed by Vario EL analyzer (Elemental Analysis Systems GmbH, Germany). The sample (2 mg) was burned at 950 °C (CHN analysis) or 1200 °C (O analysis). All analyses were repeated three times and the average C, H, N and O contents (wt%) were calculated.

The ATR-FTIR analysis of acetylation catalyzed by ZIF-90

The reaction mechanism was analyzed by ATR-FTIR (Thermo Fisher Nicolet iS50). The specific process was as follows: Firstly, PhSiH_3 (0.5 mmol) was saturated with CO_2 at 50 °C for 24 h. Then amine (0.25 mmol), ZIF-90-C (5 mol %), and PhSiH_3 (0.5 mmol) were saturated at 50 °C for 24 h. Finally, these samples obtained at different time intervals were analyzed by attenuated total reflection (ATR)-IR infrared technology.

Computational details

The B3LYP density functional method with the D3(BJ) dispersion correction was employed in this work to carry out all the computations. The 6-31G(d) basis set was used for the atoms. All structures have been optimized considering solvent effects using the PCM model for acetonitrile. Vibrational frequency analyses at the same level of theory were performed on all optimized structures to characterize stationary points as local minima or transition states. Furthermore, intrinsic reaction coordinate (IRC) computations were carried out to confirm that transition states connect to the appropriate reactants and products. The single-point energy calculations were

carried out using the def2-TZVP basis set with the M06-2X method to provide better energy correction. The Gaussian 16 suite of programs was used throughout.

Table S1. Crystallinity and crystallite size of ZIF-90 and ZIF-90-C.

Samples	Crystallinity degree (%)	Crystallite size (Dnm)
ZIF-90	87.6	46
ZIF-90-C	84.3	67

In the revised manuscript, we have supplemented the crystallinity and crystallite size (calculated by the Scherrer equation) of the two catalysts. The crystallinity and crystallite size of ZIF-90 were 87.6% and 46 nm, respectively, while that of ZIF-90-C decreased to 84.3% and 67 nm, respectively. The formation of hydrogen bond branches between-COOH in ZIF-90-C increases the length of ligands involved in crystallization, which makes the crystal plane spacing of ZIF-90-C larger, resulting in the decrease of crystallinity of ZIF-90-C.

$$\text{Crystallinity} = \frac{\text{area of crystalline peaks}}{\text{area of all peaks (crystalline + amorphous)}} \times 100\%, \quad D = \frac{k \lambda}{\beta \cos \theta}$$

k is the Scherrer constant, if β is the full width at half maximum of the diffraction peak, then $k = 0.89$; if β is the integral height and width of the diffraction peak, then $k = 1$,

D is the average thickness of the grains perpendicular to the crystal plane,

β is the measured sample diffraction peak half width (must be double-line correction and instrument factor correction), in the calculation process, need to be converted to radian (rad),

θ is the Bragg diffraction angle in angle,

λ is the wavelength of X-ray, usually 1.54056 nm.

Table S2. Surface area and porosity of ZIF-90 and ZIF-90-C.

Sample	Specific area (m ² /g)			Pore volume (m ³ /g)		Pore size (nm)
	^a S _{BET}	^b S _{micro}	^c S _{exter}	^d V _{total}	^e V _{micro}	^f D _{average}
ZIF-90	557.53	495.13	62.4	0.38	0.25	2.77
ZIF-90-C	357.22	330.98	26.24	0.29	0.17	3.35

^a The BET specific surface area of the catalyst. ^b The microporous specific surface area of the catalyst. ^c The external specific surface area of the catalyst. ^d The total pore volume of catalyst. ^e The microporous pore volume of catalyst. ^f The average pore volume of catalyst.

Table S3. Elemental analysis of ZIF-90 and ZIF-90-C.

Sample \ Element	C (%)	N (%)	O (%)	H (%)
ZIF-90	40.52	20.95	12.15	2.3
ZIF-90-C	42.41	18.93	14.56	1.8

Assuming that the increase in O content is entirely due to the formation of carboxyl groups,²¹ the amount of carboxyl groups loaded on ZIF-90-C carrier can be calculated to be 4.87 mmol/g, and the yield of aldehyde group to carboxyl group reaches 69.9%.

The formula for calculating the yield of ZIF-90-C with oxygen mass fraction is as follows:

$$\frac{B}{\frac{A}{16} \times 32 - \frac{A \times B}{16} \times 32} \times 100\% = X$$

B is the mass fraction of oxygen in ZIF-90-C, A is the mass fraction of oxygen in ZIF-90, and X is the yield of ZIF-90-C.

The formula for calculating the loading of carboxyl group on unit mass of ZIF-90-C is as follows:

$$\frac{\frac{m}{M} \times X \times 2}{m} = Z$$

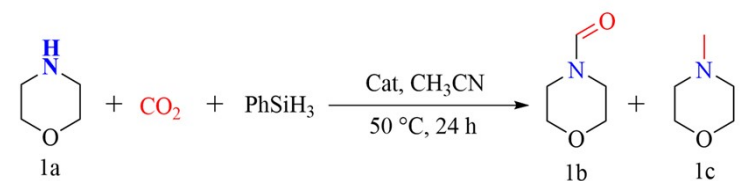
m is the mass of ZIF-90-C, M is the relative molecular mass of ZIF-90-C monomer, and Z is the loading of carboxyl group on unit mass of ZIF-90-C.

Table S4. The polarity (π^*) of different solvents.

Entry	Solvent	Polarity (π^*)
1	N,N-Dimethylformamide	0.88
2	Acetonitrile	0.66
3	Tetrahydrofuran	0.58
4	Ethyl acetate	0.55
5	Ethanol	0.54
6	<i>n</i> -hexane	-0.08

π^* is the Kamlet-Taft parameter.

Table S5. Catalytic activity of morpholine and CO₂ formylation under different silane conditions^a.



Entry	Silane	Silane dosage /mmol	Conv.(1a ,%)	Yield(1b ,%)	Yield(1c ,%)
1	PhSiH ₃	0.5	100	94	5
2	Ph ₂ SiH ₂	0.5	69	66	3
3	Et ₃ SiH	0.5	3	2	1
4	PMHS	0.5	10	8	2
5	EtO ₃ SiH	0.5	4	2	2

^a Reaction conditions: 0.25 mmol **1a**, 5 mol% ZIF-90-C, 2.0 mL CH₃CN, CO₂ balloon, 50 °C and 24 h.

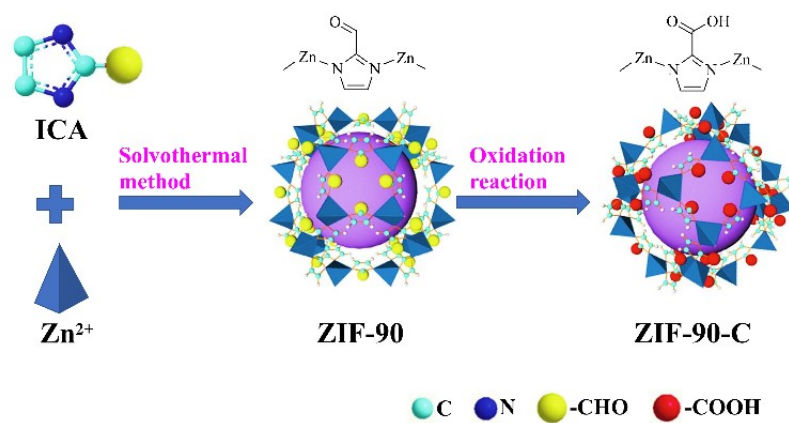


Fig. S1 Synthesis schematic of COOH-functionalized ZIF-90-C.

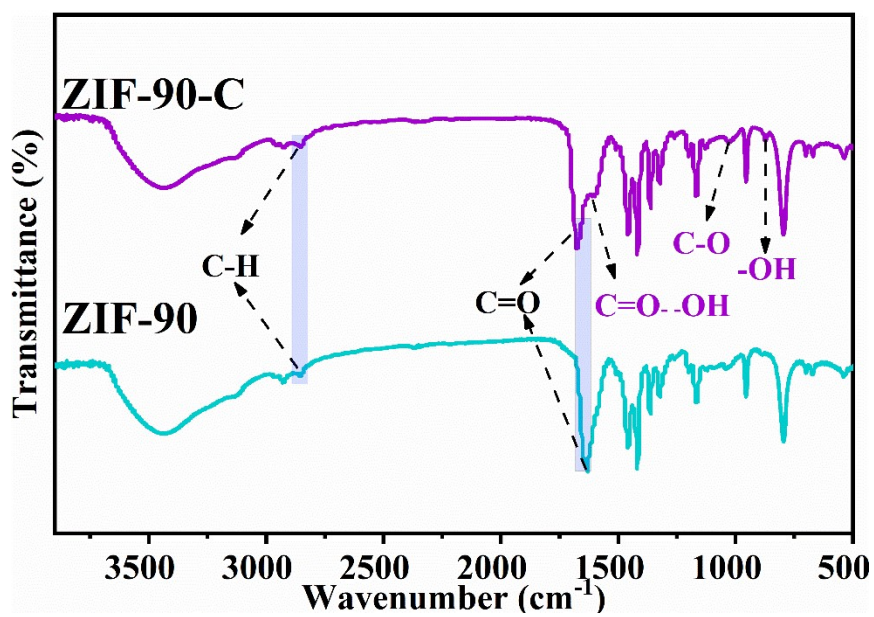


Fig. S2 FT-IR spectra of ZIF-90 and ZIF-90-C.

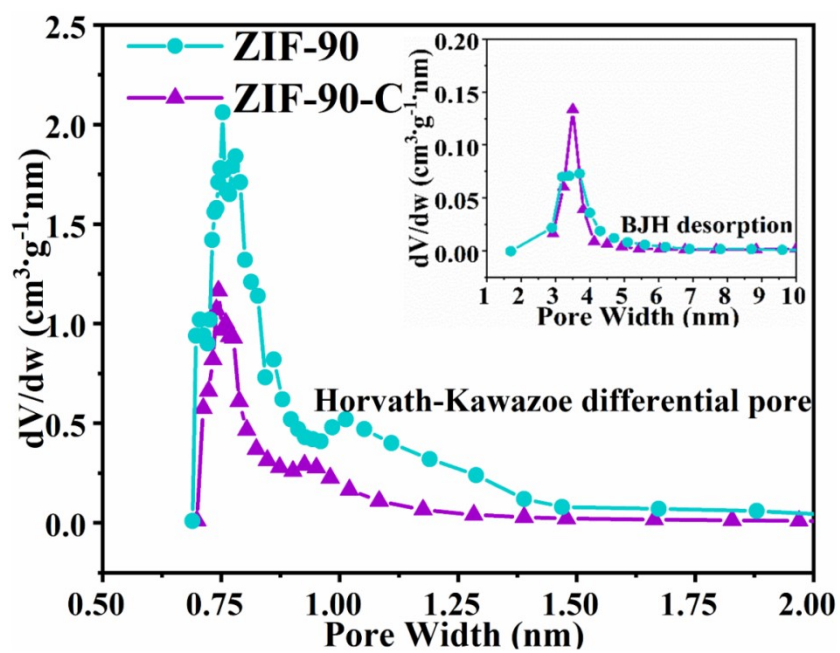


Fig. S3 Pore size distribution of ZIF-90 and ZIF-90-C.

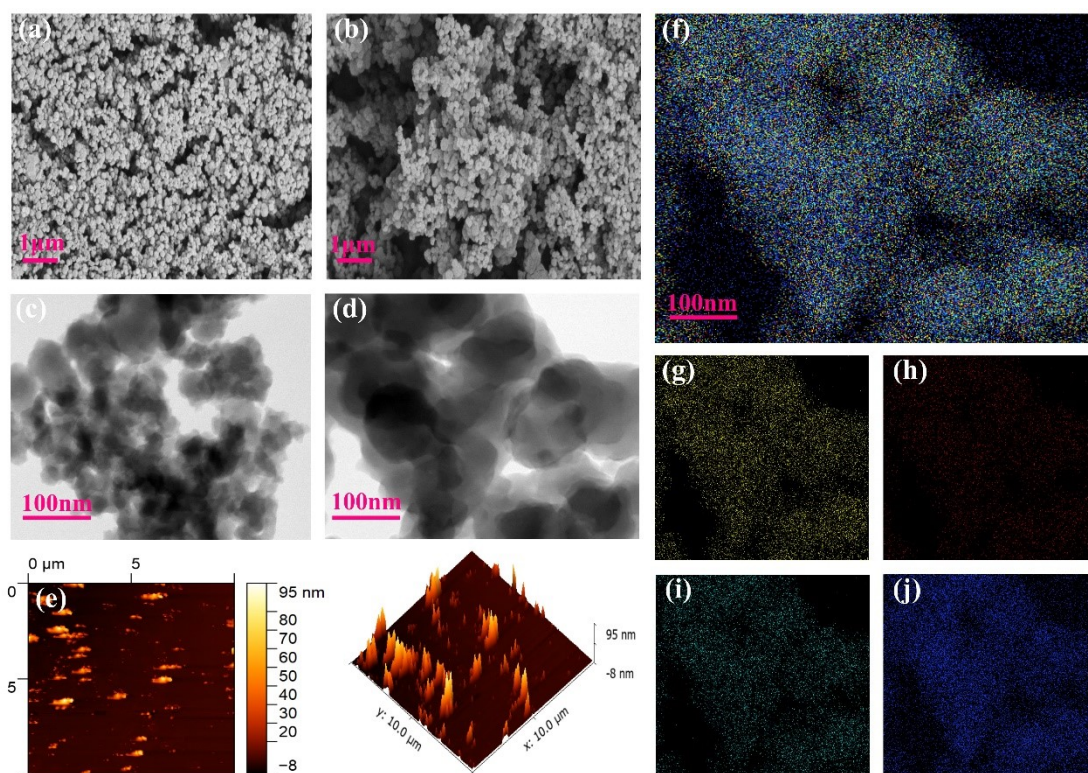


Fig. S4 SEM images: (a) ZIF-90, (b) ZIF-90-C; TEM images: (c) ZIF-90, (d) ZIF-90-C; AFM image: (e) ZIF-90-C; TEM-EDX image of (f) ZIF-90-C and elemental mapping images of (g) C, (h) O, (i) N, and (j) Zn present in ZIF-90-C.

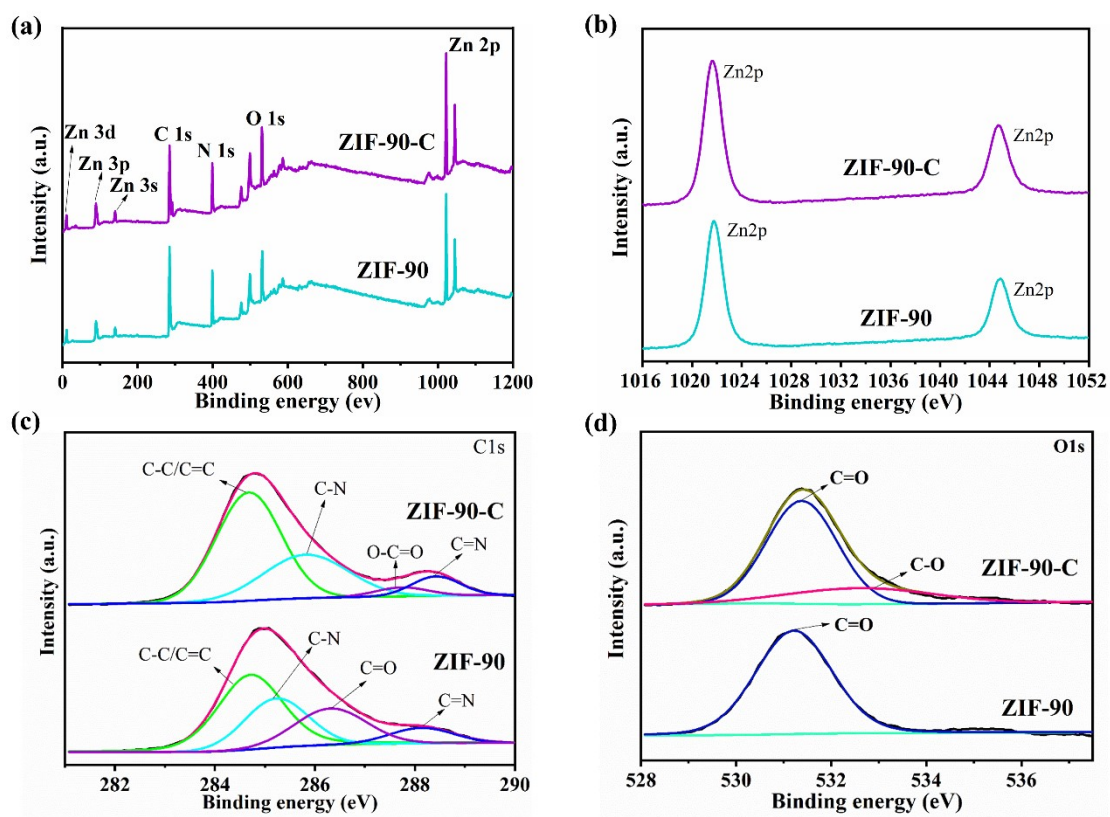


Fig. S5 (a) XPS survey spectra of ZIF-90 and ZIF-90-C; (b) C 1s spectra of ZIF-90 and ZIF-90-C; (c) O 1s spectra of ZIF-90 and ZIF-90-C; and (d) Zn 2p spectra of ZIF-90 and ZIF-90-C.

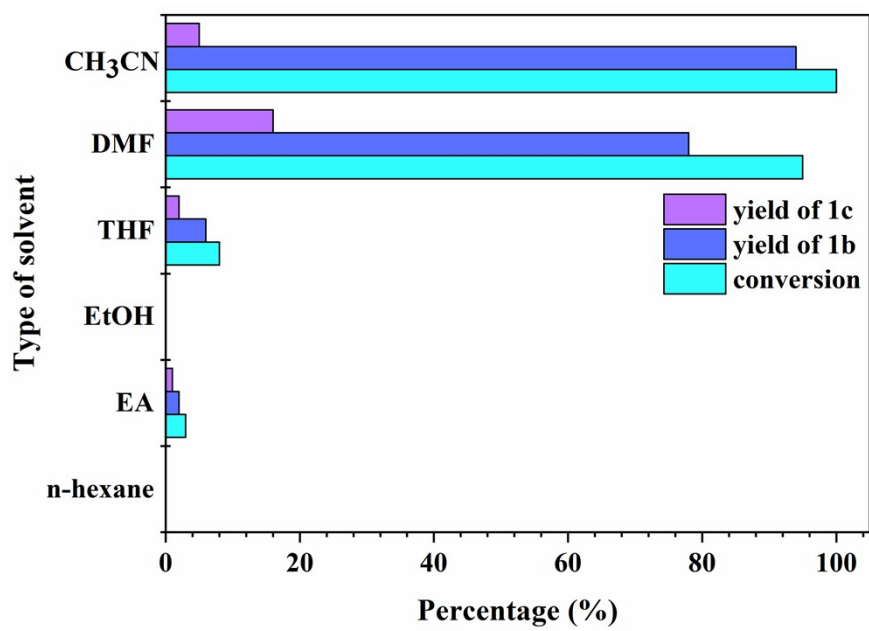


Fig. S6 The N-formylation activity of CO₂ catalyzed by ZIF-90-C using different solvents.

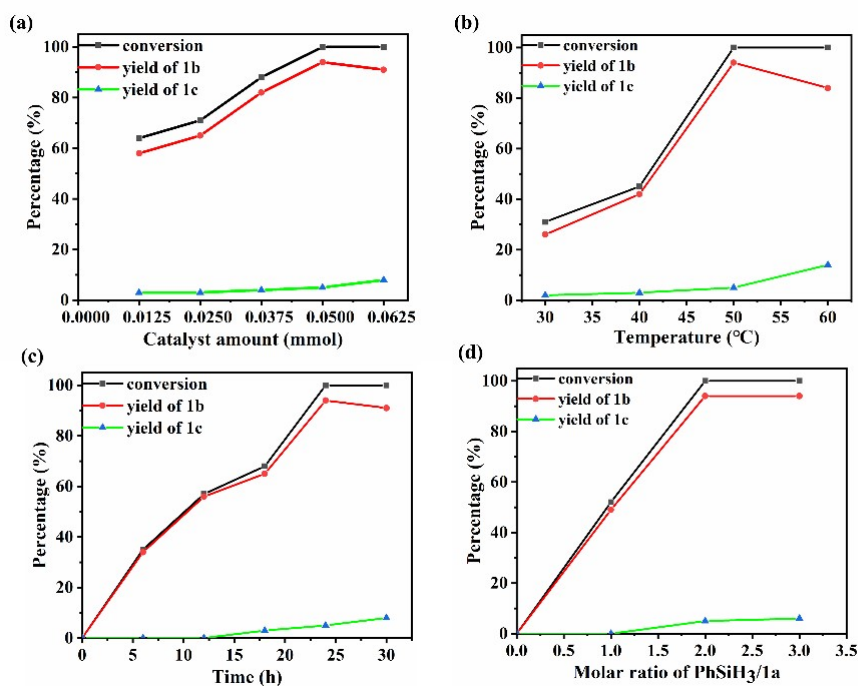


Fig. S7 Effect of (a) catalyst amount, (b) temperature, (c) reaction time, and (d) PhSiH₃ loading on reductive of CO₂ with **1a** for **1b** synthesis using ZIF-90-C. Reaction conditions: **1a**, 0.25 mmol; CH₃CN, 2 mL; [CO₂ balloon; PhSiH₃, 0.5 mmol; T, 50 °C; t, 24 h] for panel (a); [CO₂ balloon; 5 mol% catalyst; PhSiH₃, 0.5 mmol; t, 24 h] for panel (b); [CO₂ balloon; 5 mol% catalyst; PhSiH₃, 0.5 mmol; T, 50 °C] for panel (c); and [CO₂ balloon; 5 mol% catalyst; 0.5 mmol; T, 50 °C; t, 24 h] for panel (d).

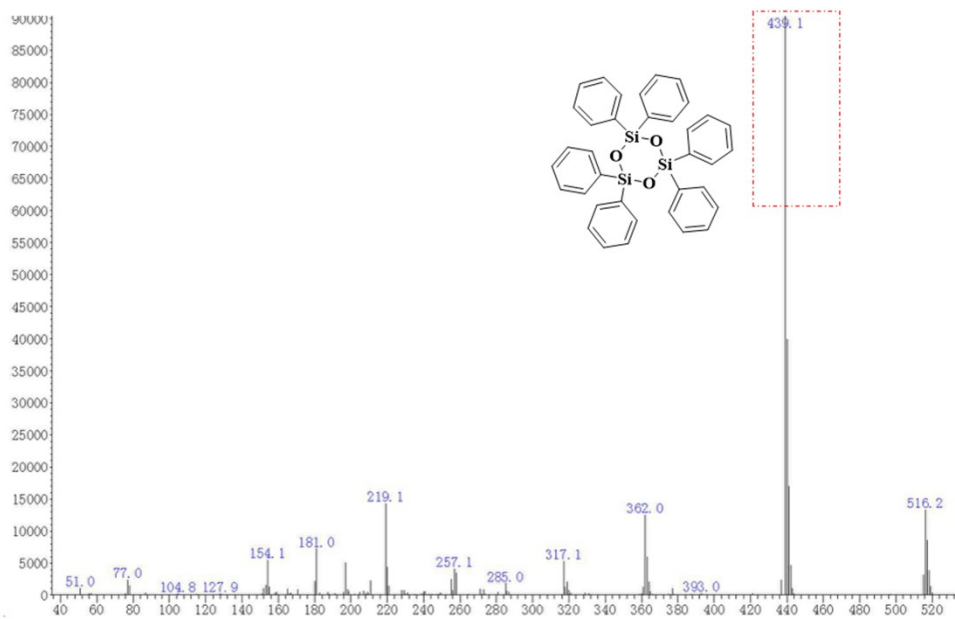


Fig. S8 The mass spectrum of the PhSiH₃ aggregation.

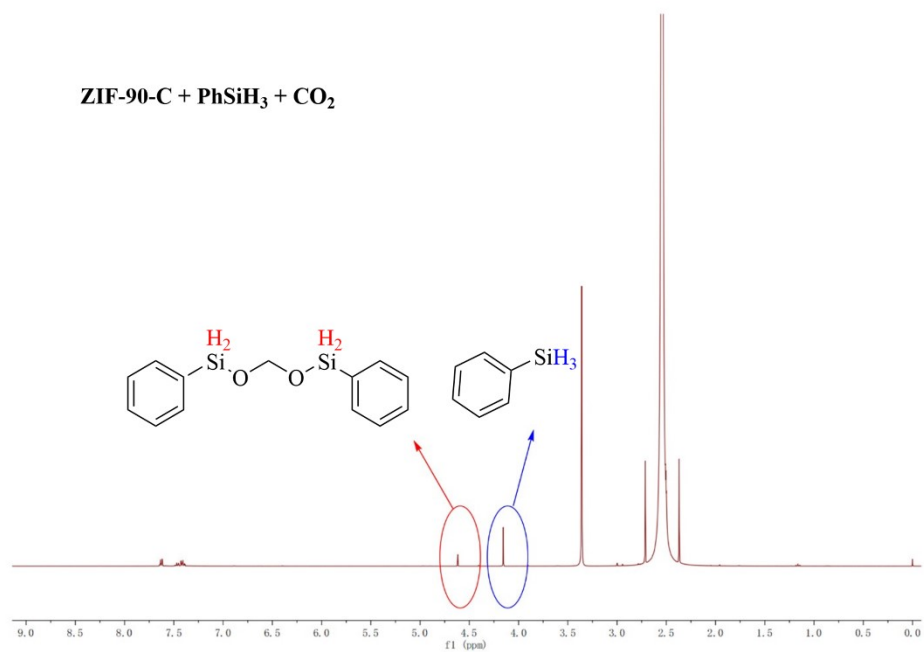


Fig. S9 ¹H NMR spectrum of CO₂ hydrosilylation without an amine (solvent: DMSO-D₆).

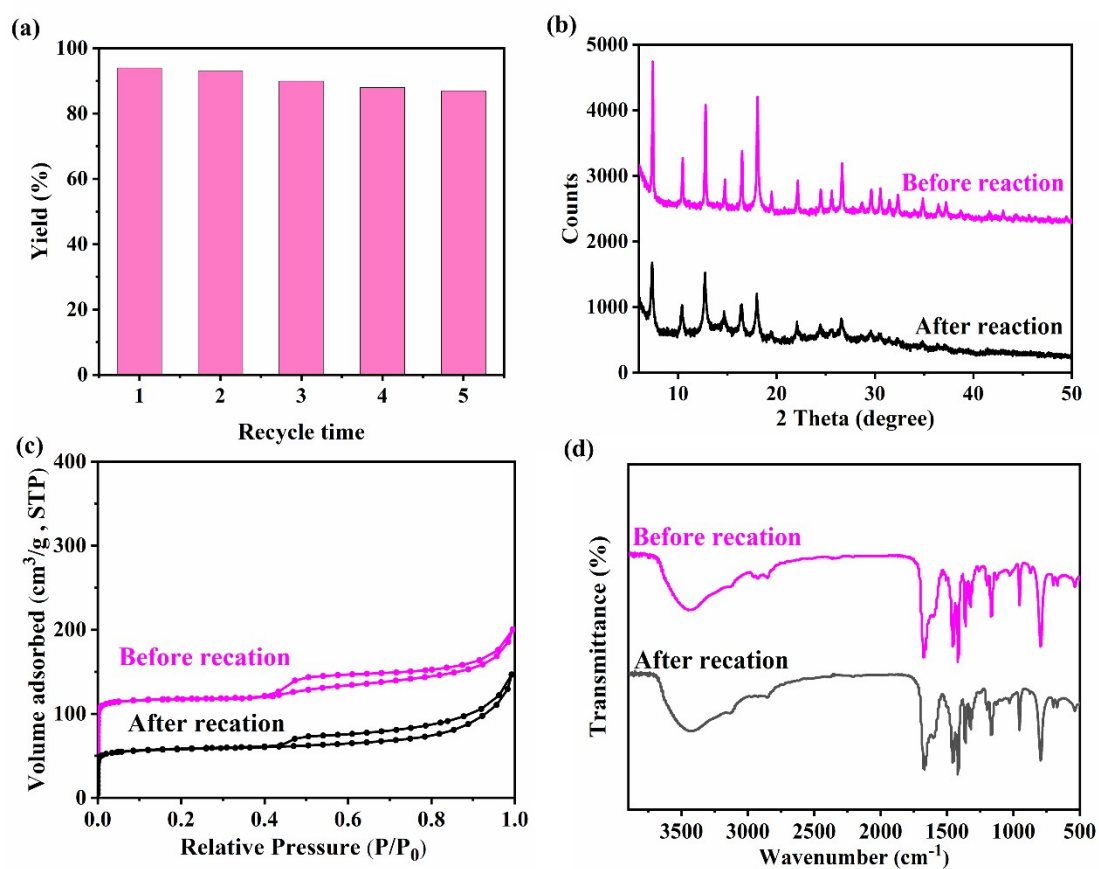


Fig. S10 (a) Study on the recyclability of catalyst ZIF-90-C; (b) XRD patterns of fresh and reused ZIF-90-C after five cycles; (c) N₂ sorption isotherms of fresh and reused ZIF-90-C after five cycles; and (d) FT-IR spectra of fresh and reused ZIF-90-C after five cycles.

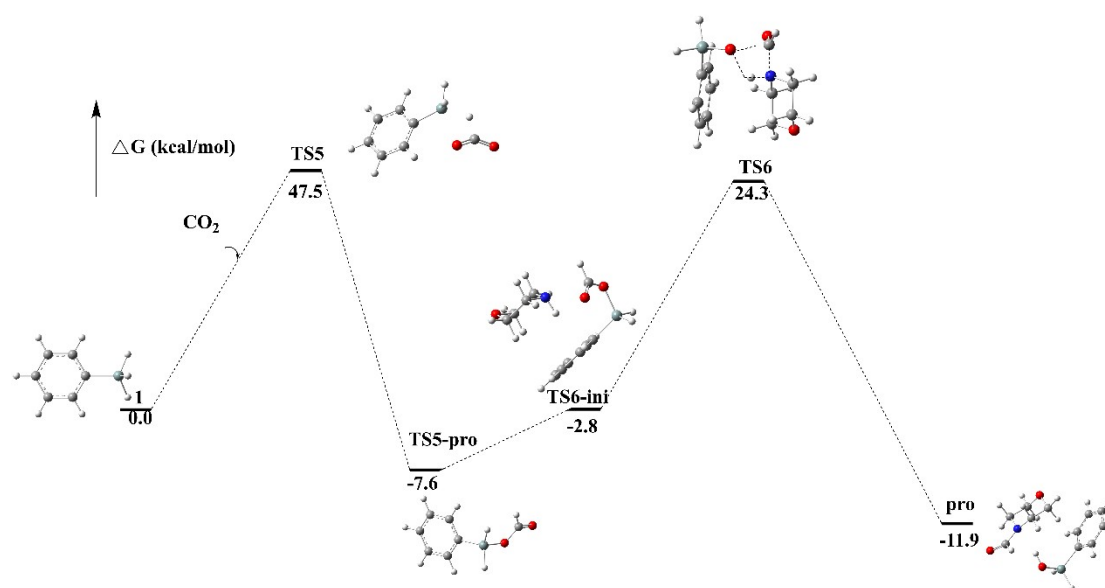


Fig. S11 Energy distribution profile of N-formylmorpholine and CO₂ reaction without catalyst

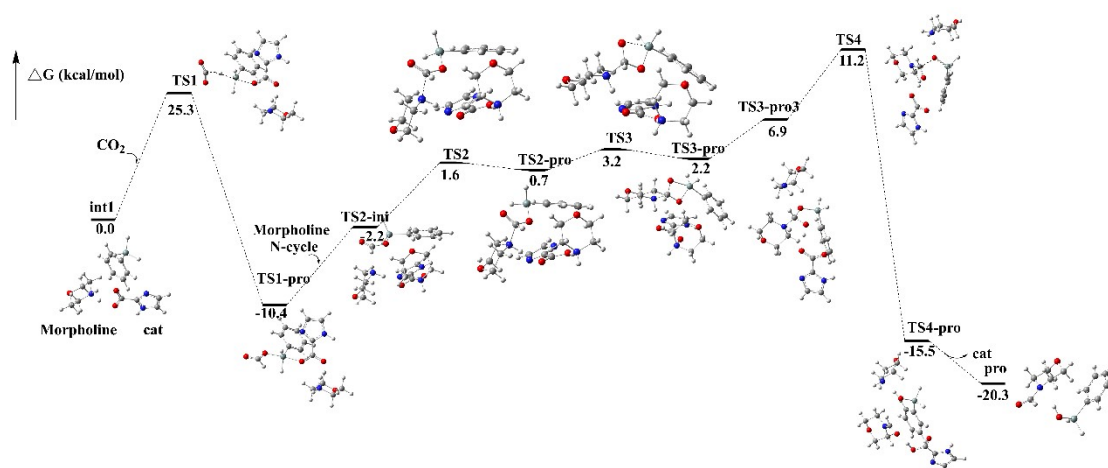


Fig. S12 Energy distribution profile of N-formylmorpholine and CO₂ reaction catalyzed by ZIF-90-C.

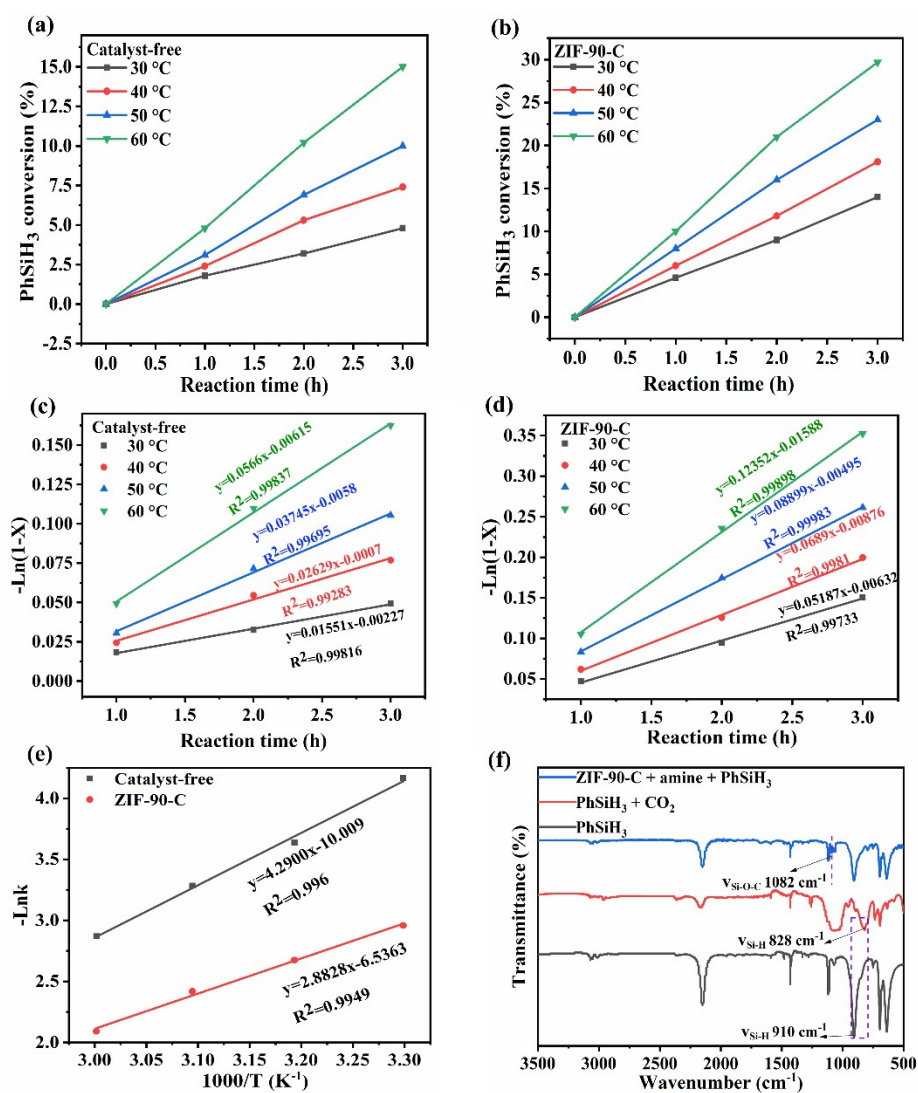


Fig. S13 The conversion rate of PhSiH₃ in PhSiH₃/CO₂-to-B at different reaction temperatures with (a) no catalyst and (b) ZIF-90-C; Kinetic plots of PhSiH₃/CO₂-to-B with (c) no catalyst and (d) ZIF-90-C; (e) Arrhenius profiles for PhSiH₃/CO₂-to-B; (f) ATR-FTIR spectra of PhSiH₃ before CO₂ absorption, after CO₂ absorption and ZIF-90-C treating with PhSiH₃. Reaction conditions: 5 mol% catalyst, 2.0 mL CH₃CN, 0.5 mmol PhSiH₃, and CO₂ balloon.

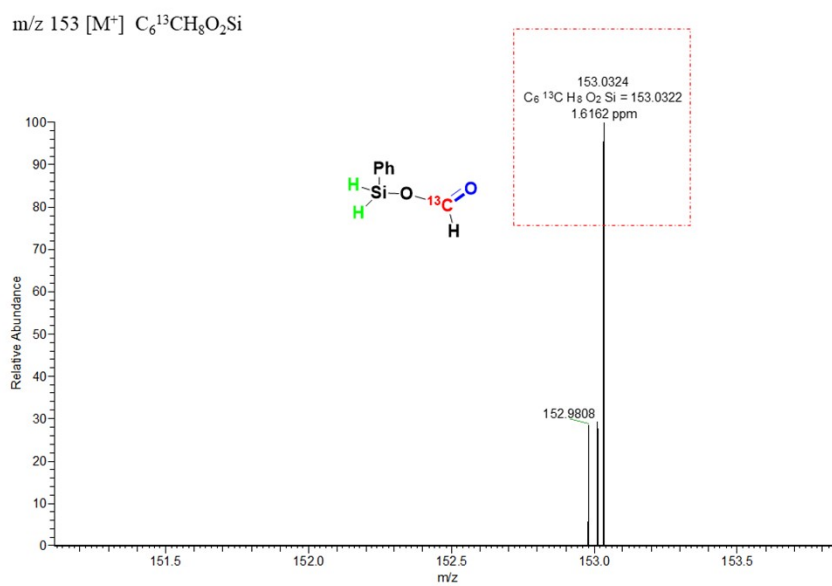


Fig. S14 HR-MS spectrum of ¹³C-labeled formoxysilane.

Reaction conditions: ¹³CO₂ balloon, morpholine (0.25 mmol), PhSiH₃ (0.5 mmol), ZIF-90-C (5 mol%), CH₃CN (2.0 mL), 50 °C and 5 h.

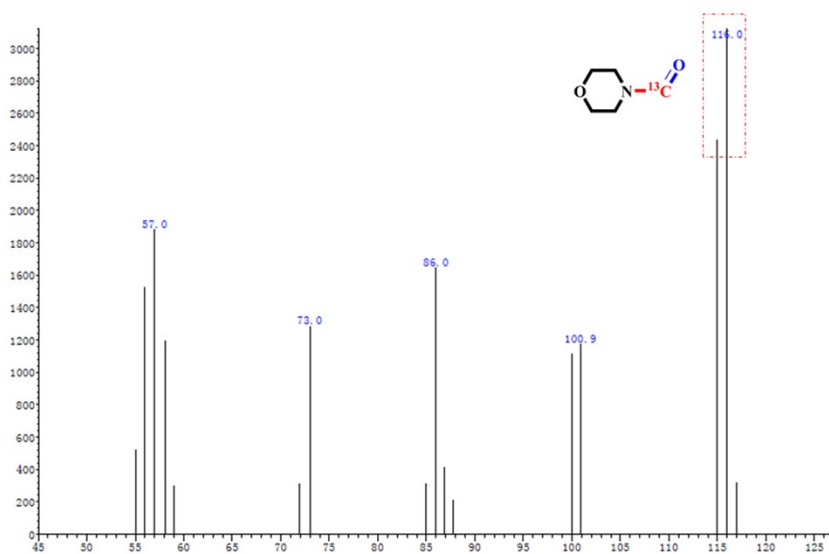


Fig. S15 GC-MS spectrum of ^{13}C -labeled N-formylmorpholine.

Reaction conditions: $^{13}\text{CO}_2$ balloon, morpholine (0.25 mmol), PhSiH_3 (0.5 mmol), ZIF-90-C (5 mol%), CH_3CN (2.0 mL), 50 °C and 5 h.

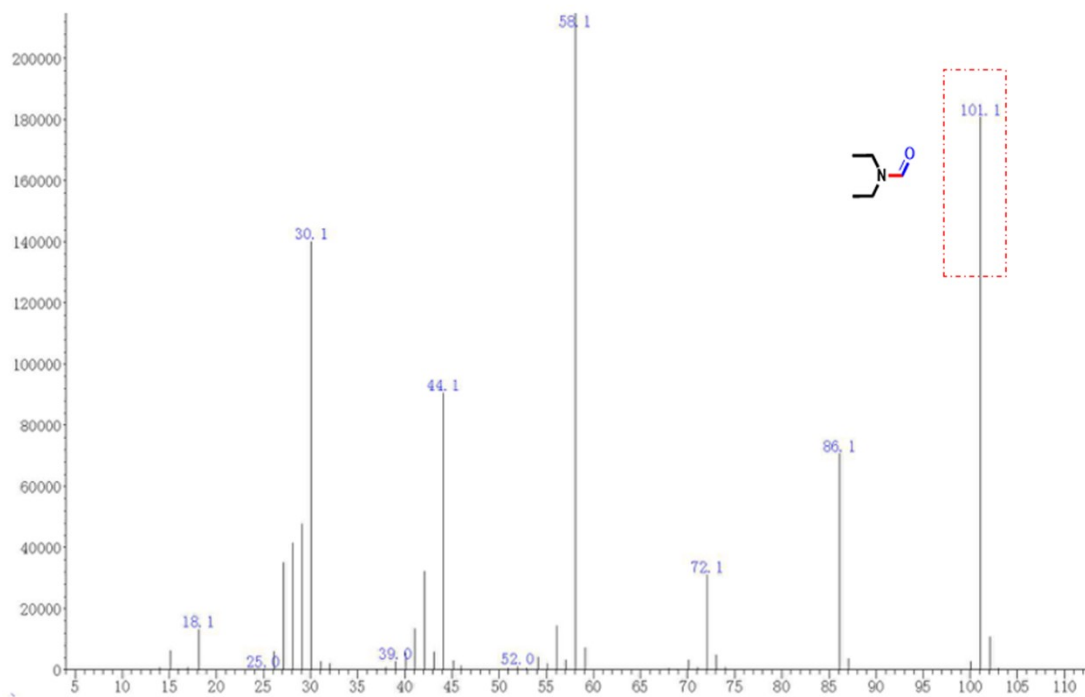


Fig. S16 The mass spectrum of **2a**.

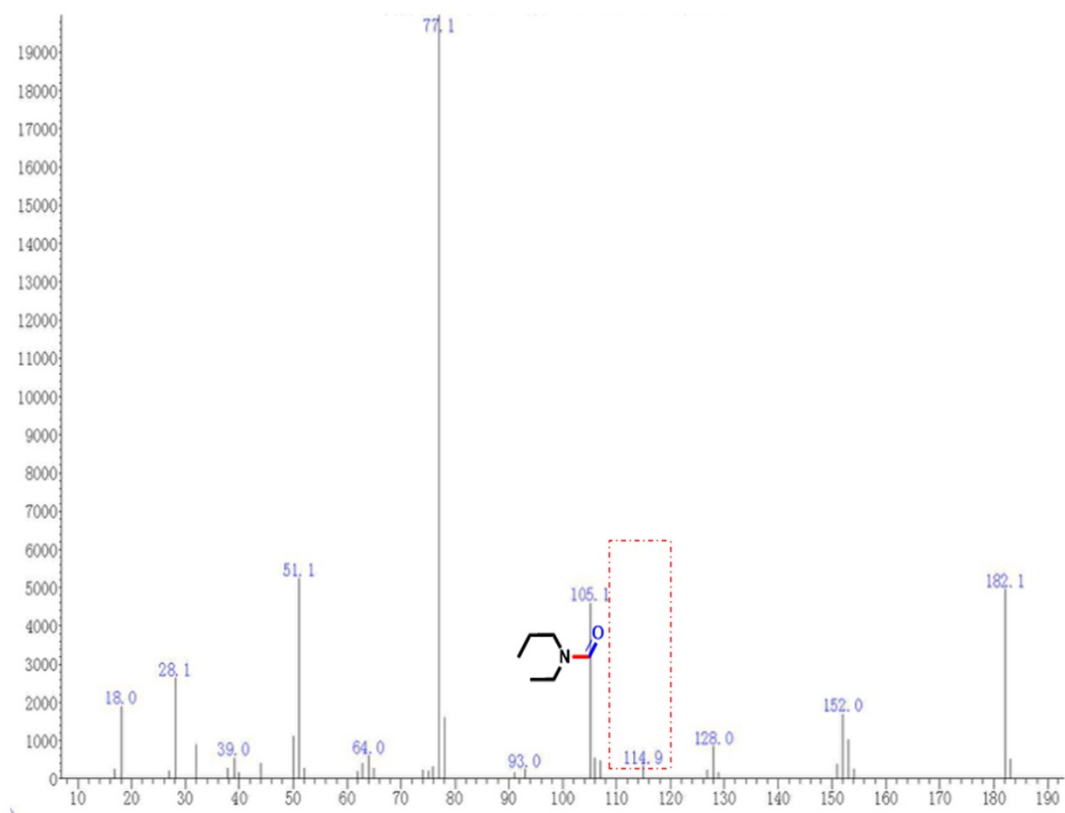


Fig. S17 The mass spectrum of **2b**.

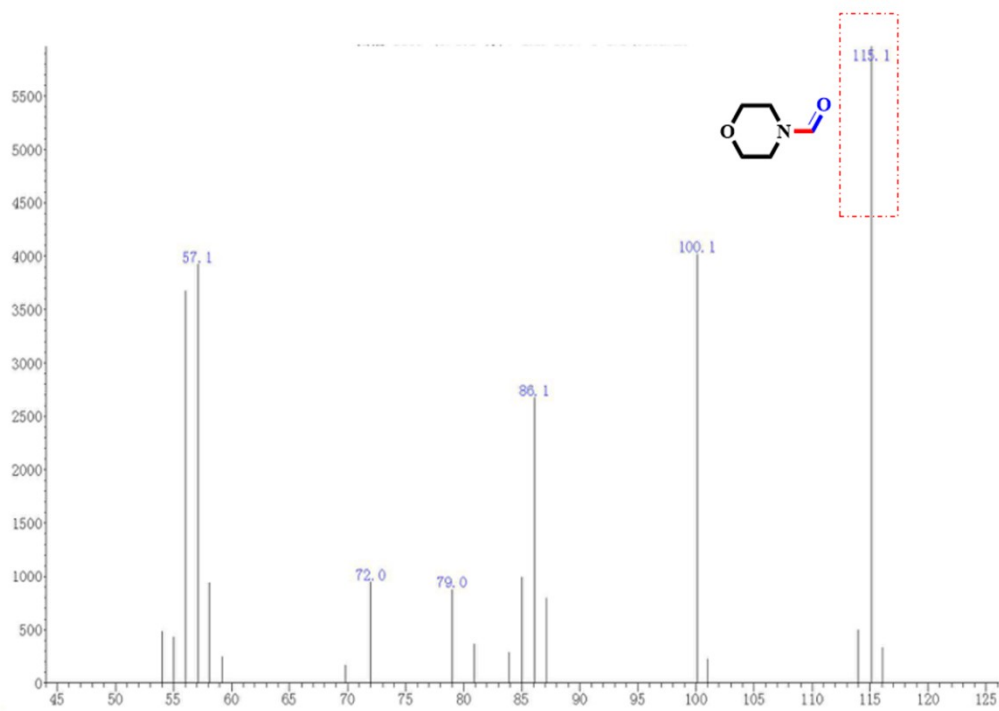


Fig. S18 The mass spectrum of **2c**.

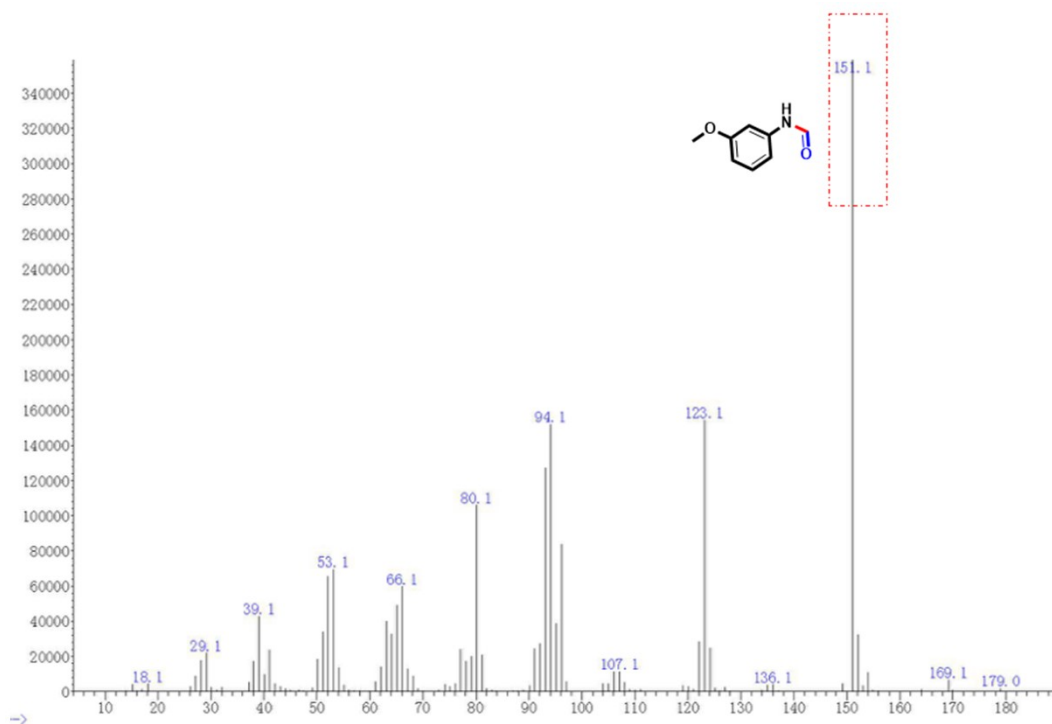


Fig. S19 The mass spectrum of **2d**.

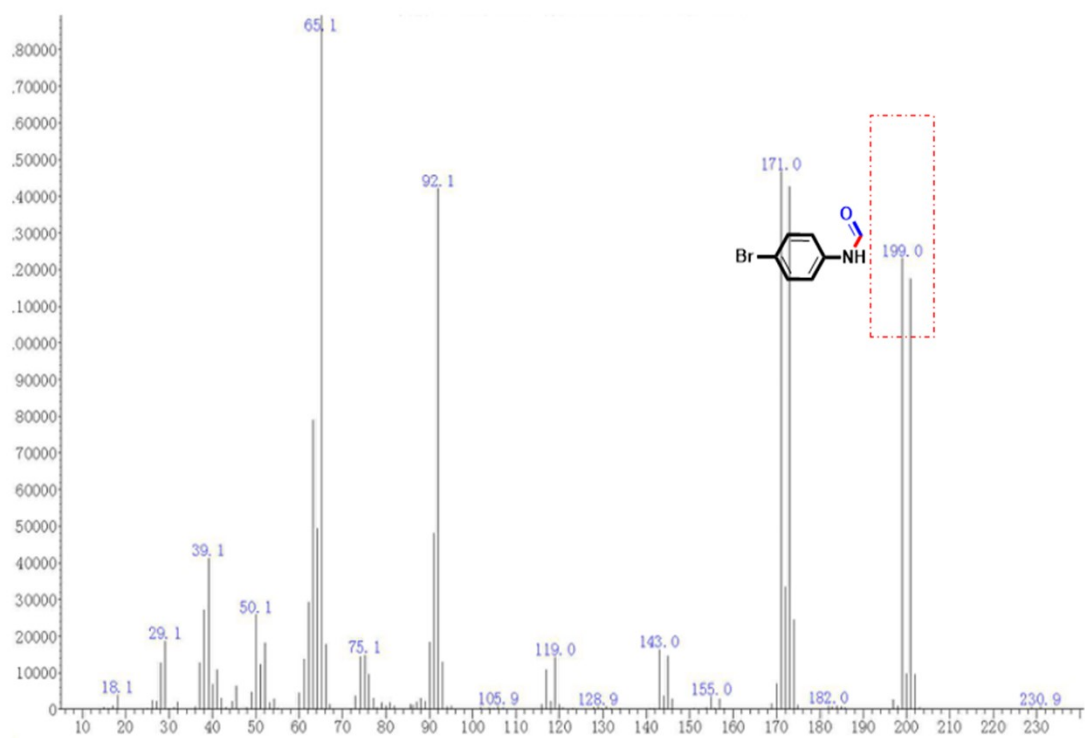


Fig. S20 The mass spectrum of **2e**.

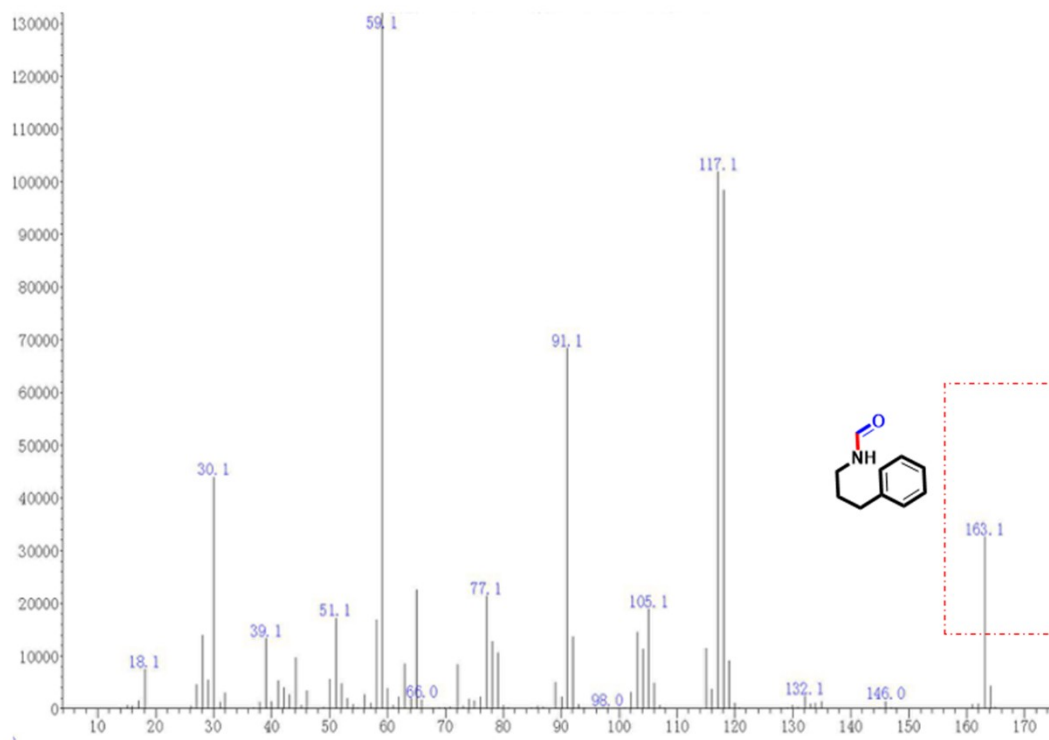


Fig. S21 The mass spectrum of **2f**.

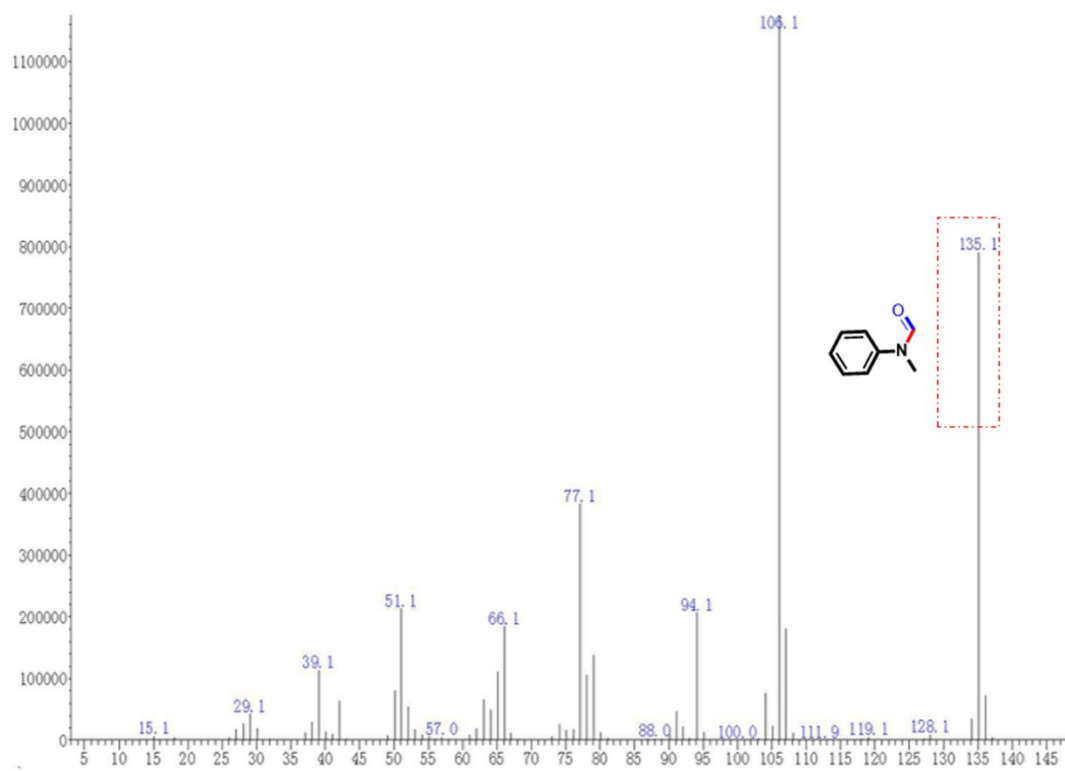


Fig. S22 The mass spectrum of **2g**.

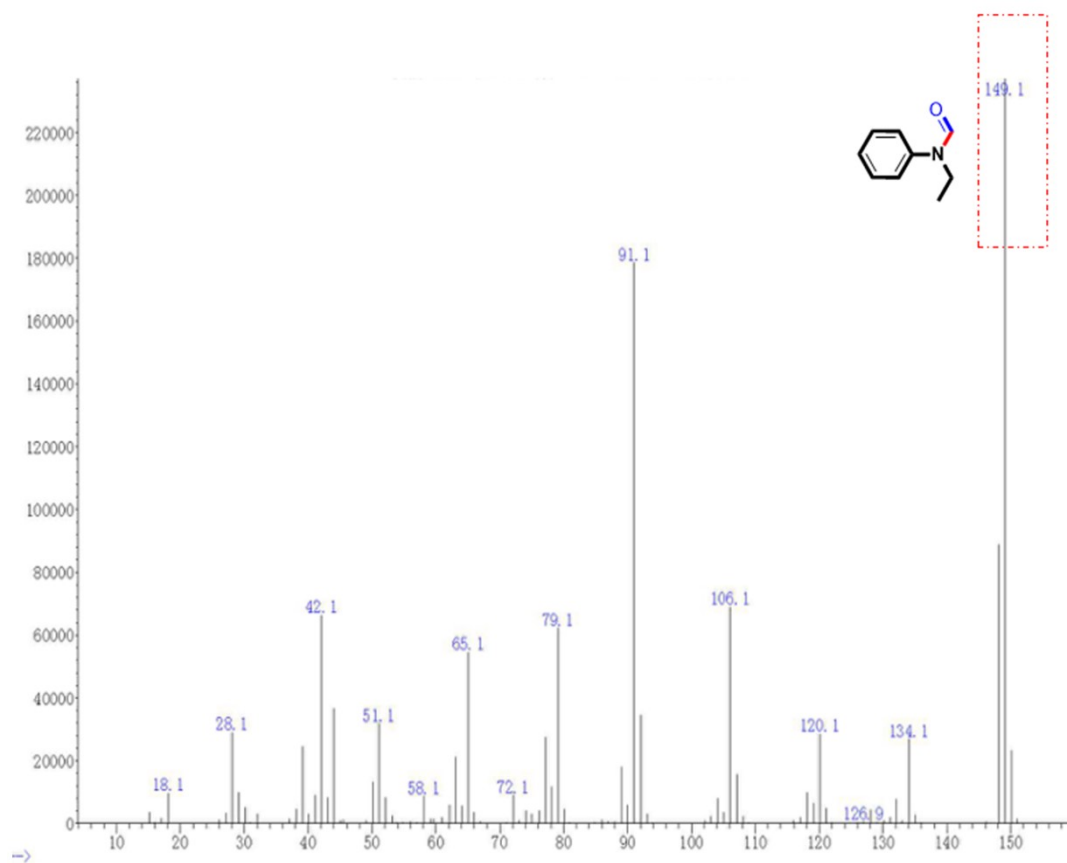


Fig. S23 The mass spectrum of **2h**.

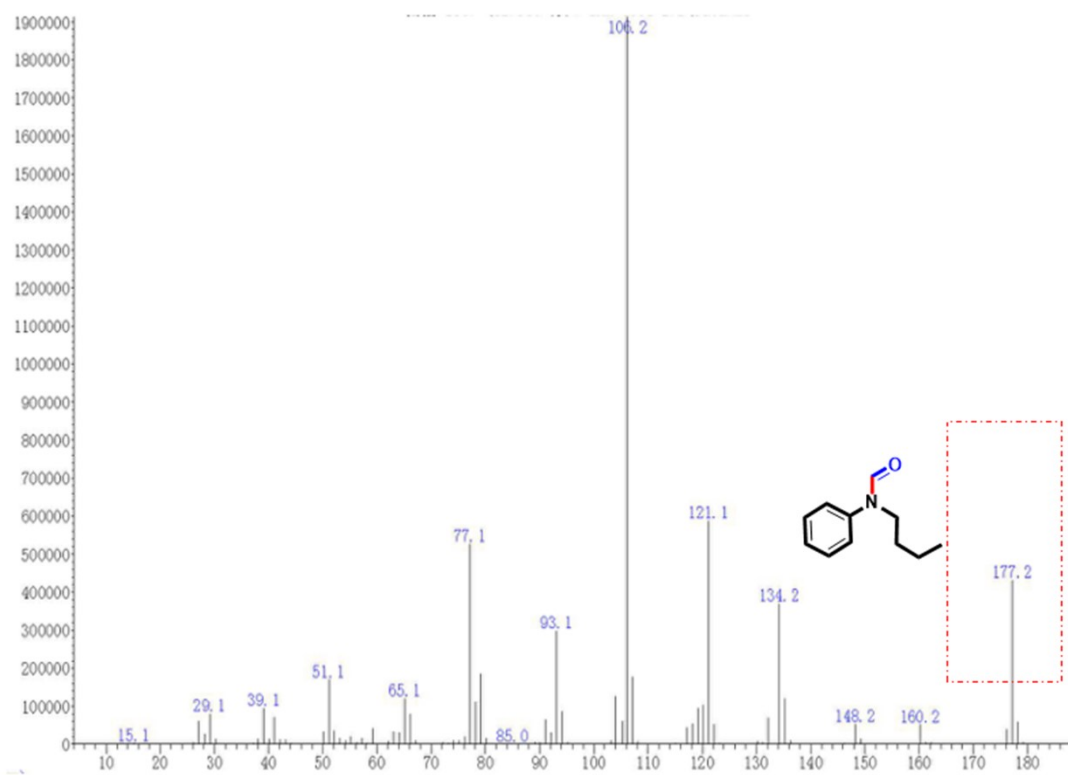


Fig. S24 The mass spectrum of **2i**.

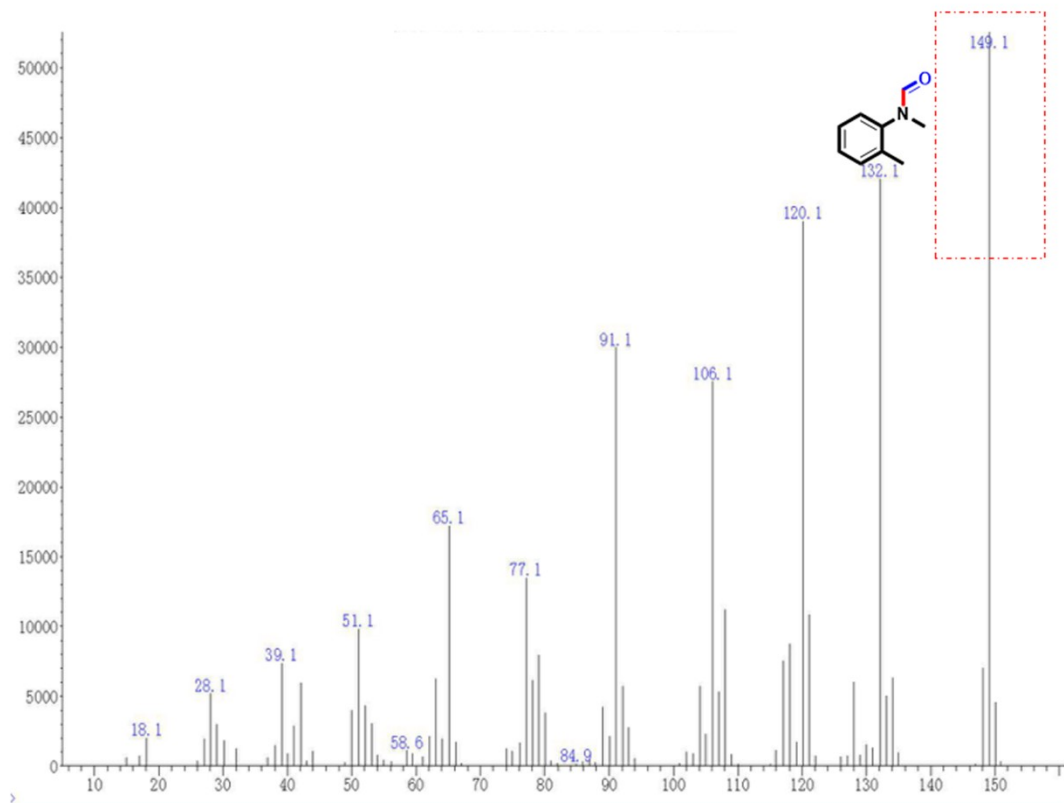


Fig. S25 The mass spectrum of **2j**.

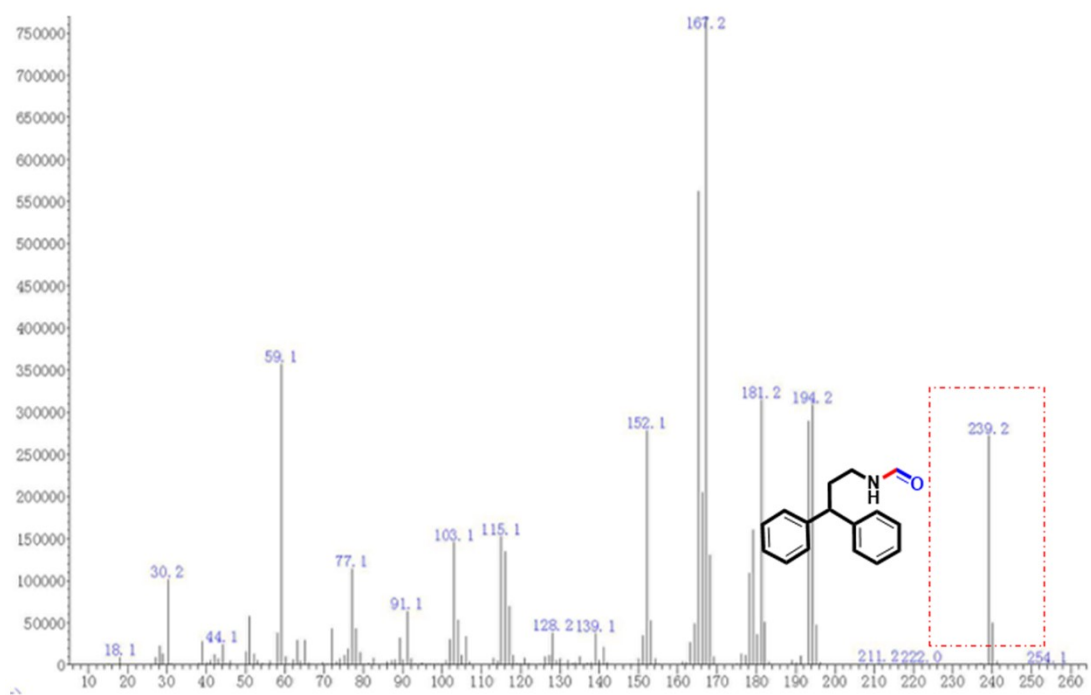


Fig. S26 The mass spectrum of **2k**.

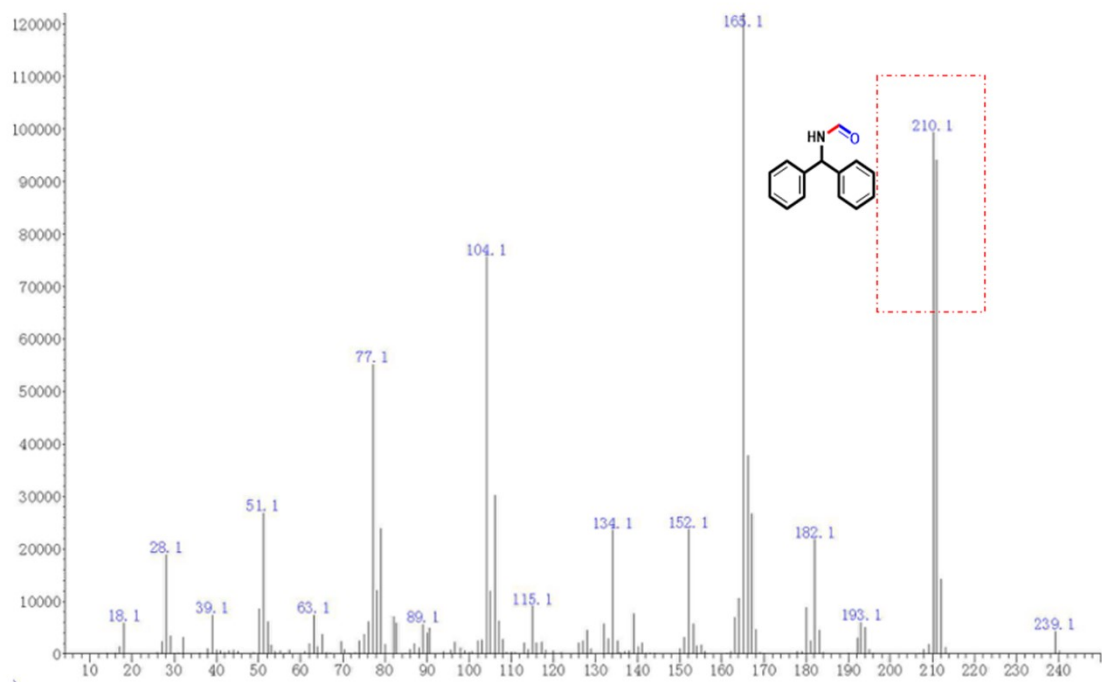


Fig. S27 The mass spectrum of **2I**.

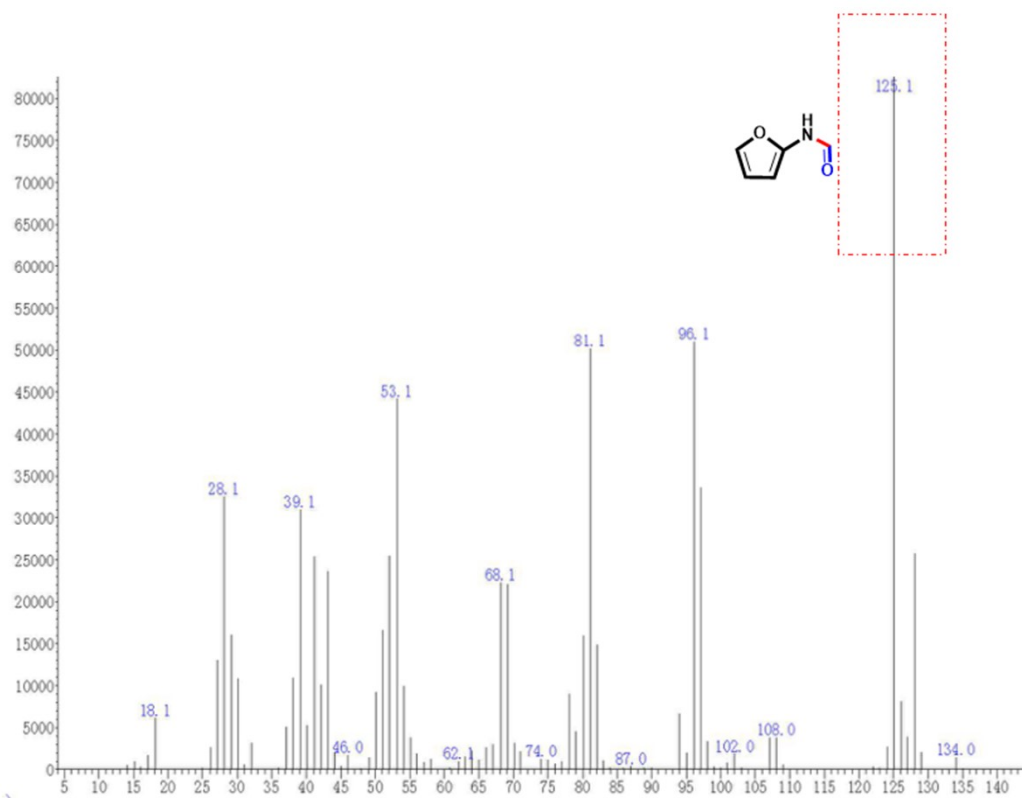


Fig. S28 The mass spectrum of **2m**.

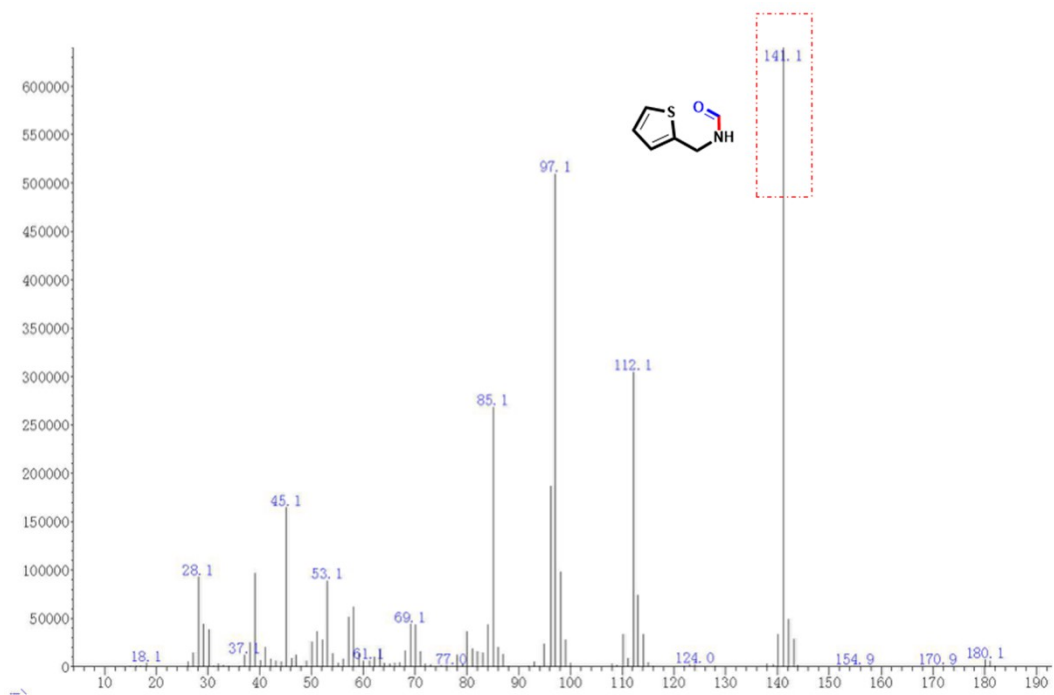


Fig. S29 The mass spectrum of **2n**.

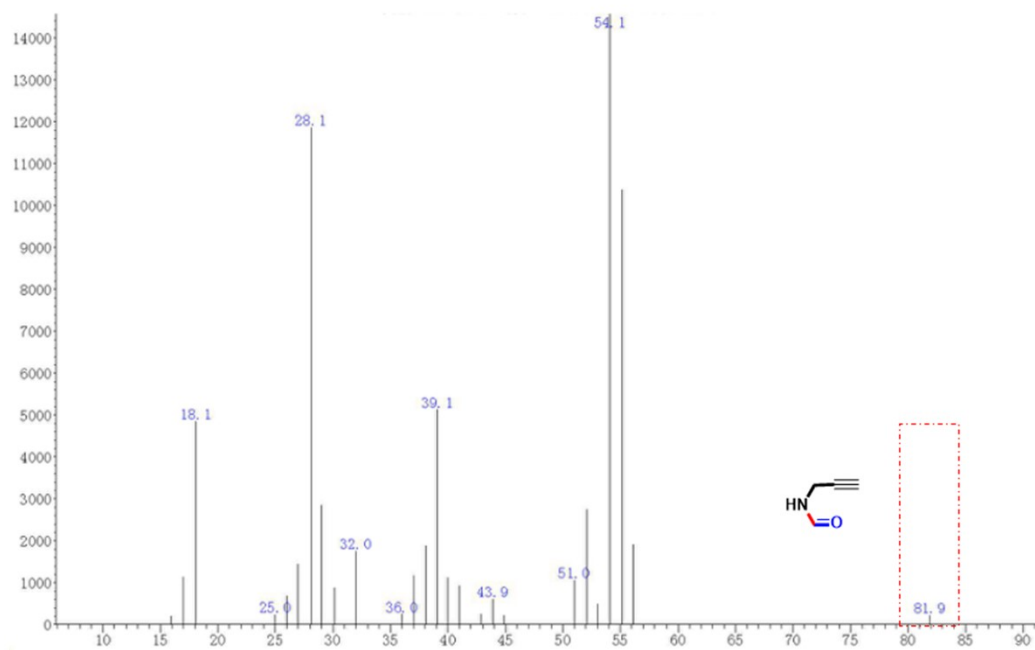


Fig. S30 The mass spectrum of **2o**.